Plant Mol Biol (2007) 65:343–355
DOI 10.1007/s11103-007-9224-1

Characterization of *Arabidopsis thaliana* genes encoding functional homologues of the yeast metal chaperone Cox19p, involved in cytochrome *c* oxidase biogenesis

Carolina V. Attallah · Elina Welchen · Claire Pujol · Geraldine Bonnard · Daniel H. Gonzalez

Received: 27 March 2007 / Accepted: 8 August 2007 / Published online: 22 August 2007

Abstract The *Arabidopsis thaliana* genome contains two nearly identical genes which encode proteins showing similarity with the yeast metal chaperone Cox19p, involved in cytochrome *c* oxidase biogenesis. One of these genes (*AtCOX19-1*) produces two transcript forms that arise from an alternative splicing event and encode proteins with different N-terminal portions. Both AtCOX19 isoforms are imported into mitochondria in vitro and are found attached to the inner membrane facing the intermembrane space. The smaller AtCOX19-1 isoform, but not the larger one, is able to restore growth on non-fermentable carbon sources when expressed in a yeast *cox19* null mutant. *AtCOX19* transcript levels increase by treatment with copper or compounds that produce reactive oxygen species. Young roots and anthers are highly stained in *AtCOX19-1::GUS* plants. Expression in leaves is only observed when cuts are produced, suggesting an induction by wounding. Infection of plants with the pathogenic bacterium *Pseudomonas syringae* pv. tomato also induces *AtCOX19* gene expression. The results suggest that *AtCOX19* genes encode functional homologues of the yeast metal chaperone. Induction by biotic and abiotic stress factors may indicate a relevant role of this protein in the biogenesis of cytochrome *c* oxidase to replace damaged forms of the enzyme or a more general role in the response of plants to stress.

C. V. Attallah · E. Welchen · D. H. Gonzalez (✉)
Cátedra de Biología Celular y Molecular,
Facultad de Bioquímica y Ciencias Biológicas,
Universidad Nacional del Litoral, CC 242 Paraje El Pozo,
Santa Fe 3000, Argentina
e-mail: dhgonza@fbcb.unl.edu.ar

C. Pujol · G. Bonnard
Institut de Biologie Moléculaire des Plantes du CNRS,
12 rue du Général Zimmer, Strasbourg cedex 67084, France

Keywords *Arabidopsis thaliana* · Biotic and abiotic stress · Copper chaperone · Cytochrome *c* oxidase biogenesis

Abbreviations

COX	Cytochrome *c* oxidase
GUS	*β*-Glucuronidase
MUG	4-Methylumbelliferyl *β*-D-glucuronide
X-gluc	5-Bromo-4-chloro-3-indolyl-*β*-D-glucuronic acid

Introduction

Complex IV or cytochrome *c* oxidase (COX), is composed of three subunits encoded in the mitochondrial genome (although one of them is nuclear-encoded in certain plants) and a variable number of subunits encoded in the nucleus (Barrientos et al. 2002). The subunits encoded within the organelle are highly conserved, constitute the catalytic core of the enzyme and have relatives in prokaryotic COX (Capaldi 1990). In addition to the polypeptides that conform the enzyme, studies using yeast mutants have revealed that several other proteins are required for the biogenesis of the complex, for the insertion of subunits into the membrane, for heme A synthesis or for the transport and insertion of metal cofactors, among other functions (Herrmann and Funes 2005; Khalimonchuk and Rödel 2005; Cobine et al. 2006).

Studies using yeast mutants with specific defects in COX revealed the existence of a protein required for COX function, termed Cox19p (Nobrega et al. 2002). Based on the presence of a conserved set of cysteine residues also observed in the metal chaperone Cox17p, involved in

copper insertion into COX subunits I and II (Glerum et al. 1996), it was postulated that Cox19p may function as a metal transporter. In spite of their similarities, Cox19p is clearly not redundant with Cox17p, since mutants in each of the corresponding genes produce defects in COX and there is no crossed complementation even when they are expressed from a multicopy plasmid (Glerum et al. 1996; Nobrega et al. 2002).

The biogenesis of the COX complex in plants is still poorly understood. We have studied the expression mechanisms of nuclear genes encoding COX subunits and found that a group of these genes is regulated by carbon and nitrogen sources, suggesting the existence of a coordinated control of expression (Welchen et al. 2002, 2004; Curi et al. 2003). To gain insight into the processes that participate in COX assembly in plants, we have also undertaken the analysis of genes encoding proteins which might be involved in the biogenesis of this complex. In this study, we report the characterization and expression analysis of *Arabidopsis thaliana* genes encoding functional homologues of yeast Cox19p, a putative metal chaperone required for COX function.

Materials and methods

Plant material and growth conditions

Arabidopsis thaliana Heyhn. ecotype Columbia (Col-0) was purchased from Lehle Seeds (Tucson, AZ). Plants were grown in a growth chamber at 22–24°C under long-day photoperiods (16 h of illumination by a mixture of cool-white and GroLux fluorescent lamps) at an intensity of approximately 200 μE m^{-2} s^{-1}. Plants used for the different treatments were grown in Petri dishes containing Murashige and Skoog medium and 0.8% agar during 3 weeks. Plants were then carefully removed from agar and incubated with the roots immersed in solutions containing the different compounds at the concentrations stated in the figure legends. During treatments plants were kept under illumination.

RNA isolation and analysis

Total RNA was isolated as described by Carpenter and Simon (1998). For northern blot analysis, specific amounts of RNA were electrophoresed through 1.5% (w/v) agarose/6% formaldehyde gels. The integrity of the RNA and equality of RNA loading were verified by ethidium bromide staining. RNA was transferred to Hybond-N nylon membranes (Amersham Corp.) and hybridized overnight at 65°C to a ^{32}P-labeled cDNA probe, comprising the entire *AtCOX19-1.1* coding region, in buffer containing 6 × SSC, 0.1% (w/v) polyvinylpirrolidone, 0.1% (w/v) BSA, 0.1% (w/v) Ficoll, 0.2% (w/v) SDS, and 10% (w/v) polyethylene glycol 8000. Filters were washed with 2 × SSC plus 0.1% (w/v) SDS at 65°C (4 times, 15 min each), 0.1 × SSC plus 0.1% (w/v) SDS at 37°C during 15 min, dried and exposed to Kodak BioMax MS films. To check the amount of total RNA loaded in each lane, filters were then re-probed with a 25S rDNA from *Vicia faba* under similar conditions as those described above, except that hybridization was performed at 62°C and the wash with 0.1 × SSC was omitted.

RT-PCR analysis was performed on RNA samples prepared as described above. First strand cDNA synthesis was performed using primer 19-2 (5′-AGGCTCGATATGAGTACAG-3′) and MMLV reverse transcriptase (Promega) under standard conditions. PCR was performed on an aliquot of the cDNA synthesis reaction with primers 19-1 (5′-CATCAAGTTCTTAGCCATTC-3′) and 19-2 using cycles of 60 s at 94°C, 45 s at 56°C and 90 s at 72°C. Aliquots of the reaction were removed after 15, 25 and 35 cycles and analyzed by agarose gel electrophoresis followed by transfer and hybridization to an *AtCOX19-1.1* probe.

Complementation of a yeast *cox19* mutant with AtCOX19-1 cDNAs

For complementation of a yeast *cox19* mutant strain, the coding regions of both transcript variants from the *AtCOX19-1* gene were inserted in both orientations into the *Eco*RI site of the yeast expression vector pYPGE15, containing a *PGK* promoter and a *CYC1* terminator (Brunelli and Pall 1993). For this purpose, *AtCOX19-1* variant 1 was amplified from an Arabidopsis full-length cDNA clone (RAFL19-72-F12, accession no. AK118487, obtained from the RIKEN BRC Experimental Plant Division, Japan), using primers 19-3 (5′-GGCAAGCTTTACAAAGATGAGTACAGGTGGAGCA-3′) and 19-5 (5′-GGCAAGCTTTCTTTTGTCAACCTTTCA-3′) and cloned into vector pCR2.1-TOPO (Invitrogen). A clone encoding *AtCOX19-1* splice variant 2 in pCR2.1-TOPO was obtained in a similar way by reverse transcription followed by PCR on total RNA using specific oligonucleotides 19-4 (5′-GGCAAGCTTTACAAAGATGATCACTATAAAGTTCG-3′) and 19-5. The corresponding inserts were excised with *Eco*RI from pCR2.1-TOPO and cloned into pYPGE15. Clones with inserts in both orientations and the empty plasmid were introduced into the yeast *cox19* null mutant strain aW303ΔCOX19H (MATa *ade2-1 his3-1,15 leu2-3,112 trp1-1 ura3-1*, *cox19::HIS3*; Nobrega et al. 2002), kindly provided by Alexander Tzagoloff (Columbia University, New York), using the standard lithium acetate

transformation method. Clones able to grow on minimal medium without uracil were checked for the presence of the plasmid by PCR and then tested for growth on fermentable (YPD: 2% glucose, 1% yeast extract, 2% peptone) or non-fermentable (YEPG: 3% glycerol, 2% ethanol, 1% yeast extract, 2% peptone) media. The parent strain W303-1A (MATa *ade2-1 his3-1,15 leu2-3,112 trp1-1 ura3-1*) was used as a positive control of growth.

Import of radiolabeled proteins into isolated mitochondria

[^{35}S]methionine labelled COX19 proteins were synthesized from the corresponding cDNA clones by coupled transcription/translation according to the supplier's instructions (Promega). The haemoglobin from the reticulocyte lysate interferes with the electrophoretic analysis of small sized proteins tested in import experiments. Therefore, the proteins were precipitated with ammonium sulfate (66% saturation) as described in Diekert et al. (2001). Mitochondria were purified from potato tubers and used for import experiments as described in Duchêne et al. (2001). Swollen mitochondria were obtained by resuspending mitochondria in 10 mM potassium phosphate, pH 7.5, and incubated on ice during 20 min to disrupt the outer membrane. After import, intact or swollen mitochondria were treated with 100 μg/ml proteinase K (PK) for 10 min at 4°C as indicated. Some import reactions were performed in the presence of 2 μM valinomycin (Val) for 10 min at 4°C or treated with 1% Triton X-100 after import as indicated. Phenylmethylsulfonyl fluoride was added at the final concentration of 1 mM to stop the protease activity, and the organelles were recovered by centrifugation through a 22% sucrose cushion at 15,000*g* for 15 min. Mitochondria were resuspended in 10 mM potassium phosphate, pH 7.5, and broken by three freeze/thaw cycles. The membrane and soluble fractions were separated by a 15-min centrifugation at 100,000*g* in a Beckman TLA-100 rotor.

Reporter gene construct and plant transformation

A 1.5-kbp *Hin*dIII/*Bgl*II fragment, comprising non-transcribed upstream sequences, exon 1, intron 1 and part of exon 2 from *AtCOX19-1*, was amplified from Arabidopsis genomic DNA using oligonucleotides 5′-GGCAAGC TTTTTTCAGGGGATTCACTAA-3′ and 5′-GCGAGAT CTGTCCTCTGTTTCCTCCAAA-3′ and cloned in frame with the *gus* coding region into plasmid pBI101.3 digested with *Hin*dIII and *Bam*HI. The construct was introduced into *Agrobacterium tumefaciens* strain GV2260, and transformed bacteria were used to obtain transgenic Arabidopsis plants by the floral dip procedure (Clough and Bent 1998). Transformed plants were selected on the basis of kanamycin resistance and positive PCR carried out on genomic DNA with primers specific for *AtCOX19-1* and the *gus*-specific primer 5′-TTGGGGTTTCTACAG GAC-3′. Ten independent lines were further reproduced and homozygous T3 and T4 plants were used to analyze *gus* expression. Plants transformed with pBI101.3 were obtained in a similar way and used as negative control of expression.

β-Glucuronidase assays

β-Glucuronidase (GUS) activity of transgenic plants was analysed by histochemical staining using the chromogenic substrate 5-bromo-4-chloro-3-indolyl-β-D-glucuronic acid (X-gluc) as described by Hull and Devic (1995). Whole plants or separated organs were immersed in a 1 mM X-gluc solution in 100 mM sodium phosphate, pH 7.0, and 0.1% Triton X-100 and, after applying vacuum for 5 min, they were incubated at 37°C during 1.5 h or overnight. Tissues were cleared by immersing them in 70% ethanol.

Specific GUS activity in protein extracts was measured using the fluorogenic substrate 4-methylumbelliferyl β-D-glucuronide (MUG) essentially as described by Jefferson et al. (1987). Total protein extracts were prepared by grinding the tissues in extraction buffer (50 mM sodium phosphate, pH 7.0, 10 mM EDTA, 10 mM β-mercaptoethanol) containing 0.1% (w/v) SDS and 1% Triton X-100, followed by centrifugation at 13,000*g* for 10 min. GUS activity in supernatants was measured in extraction buffer containing 1 mM MUG and 20% methanol. Reactions were stopped with 0.2 M Na_2CO_3 and the amount of 4-methylumbelliferone was calculated by relating relative fluorescence units with those of a standard of known concentration. The protein concentration of extracts was determined as described by Sedmak and Grossberg (1977).

Treatments were performed by vacuum infiltration (15 min in a desiccator) of excised rosette leaves suspended in solutions containing the different compounds at the concentrations stated in the figure legends. Effectors were dissolved in water (used as control of infiltration). During treatments, leaves were kept under illumination and gentle agitation. *Pseudomonas syringae* pv. tomato DC3000 (with or without the *avrRpm1* gene) was grown as described (Alvarez et al. 1998). After washing and resuspension in a solution containing 1 mM $MgCl_2$, leaves were subjected to vacuum infiltration as described above. A 1 mM $MgCl_2$ solution was used for infiltration of control leaves. Treatment of whole plants with copper solutions was performed on plants grown on vermiculite for 10 days.

Plants were irrigated with $CuSO_4$ at different concentrations during 2 days before GUS expression was analyzed.

Results

Identification of two *COX19* genes in Arabidopsis

A search for *COX19* homologous genes in the Arabidopsis genome using the program tblastn identified two candidate genes with homology with yeast *COX19*, both located in chromosome 1. Both genes are expressed, since cDNA clones (either EST or full-length) could be identified. Therefore, the corresponding genes were named *AtCOX19-1* and *AtCOX19-2* (for At1g66590 and At1g69750, respectively). *AtCOX19-1* and *AtCOX19-2* are composed of four exons and have the capacity to encode identical proteins. Within non-coding regions the level of identity is very high, with only 18 changes within introns and 4 changes within exon untranslated regions. This suggests that these two genes arose from a very recent duplication of the Arabidopsis genome which extends far beyond the coding region.

For *AtCOX19-1*, two cDNAs differing in their 5′ region were found which most likely arise from an alternative splicing event originated from the use of two different acceptor sites during intron 1 splicing (Fig. 1A). As a consequence, a start codon is out of frame in one of the splice variants, and a downstream ATG is used to initiate translation. This generates proteins with different N-terminal regions. Accordingly, these two splice variants, which were named *AtCOX19-1.1* and *AtCOX19-1.2*, encode proteins of 98 and 113 amino acids, respectively.

We have not detected splice variants from the second gene, which is noteworthy, considering its high similarity with *AtCOX19-1*. In this case, the sequence corresponding to splice variant 2 would contain a deletion of 2 nucleotides, thus producing a frameshift soon after the start codon. Accordingly, if this splice variant is produced from *AtCOX19-2* it must be rapidly degraded by the nonsense-mediated mRNA decay pathway (Baker and Parker 2004).

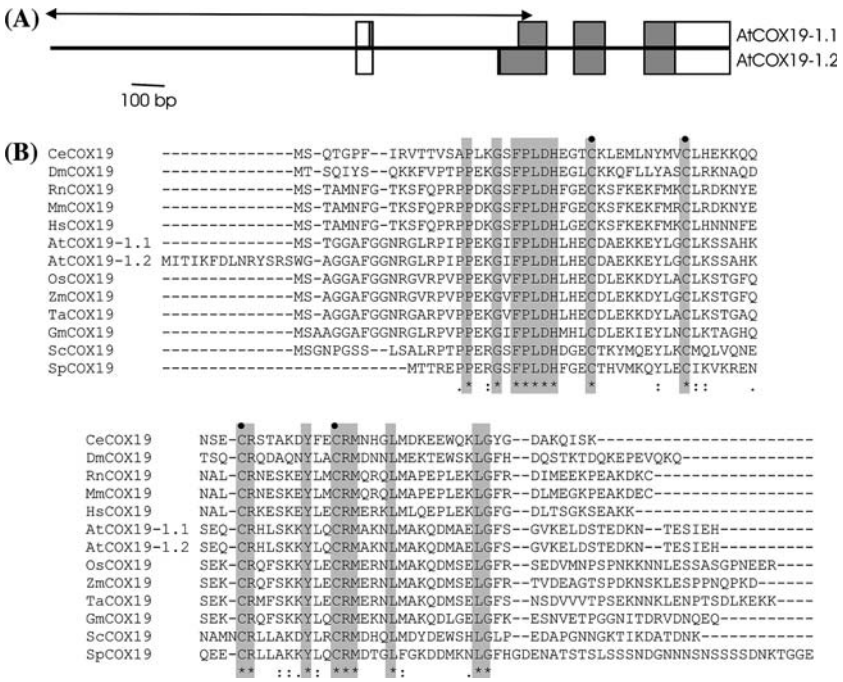

Fig. 1 Alternative splicing of the *AtCOX19-1* gene produces transcripts with different coding capacity. (**A**) Scheme of the *AtCOX19-1* (At1g66590) gene. Coding and non-coding exon regions that give rise to AtCOX19-1.1 and AtCOX19-1.2 are denoted by grey and white boxes, respectively. The arrow indicates the fragment that was fused to the *gus* coding region for expression studies. (**B**) Alignment of COX19 proteins from different organisms. Sequences encoding homologues of yeast COX19p were retrieved from data banks using the program tblastn. Protein sequences were aligned using ClustalW (Thompson et al. 1994). Positions occupied by identical amino acids are shaded and marked with an asterisk; those occupied by related amino acids are marked with double-dots. Positions with several conserved amino acids are marked with a single dot. Cysteines of conserved Cx_9C motifs are identified with black circles. The sequences used for the analysis are from *Caenorhabditis elegans* (CeCOX19, NM_060318), *Drosophila melanogaster* (DmCOX19, AY102691) *Rattus norvegicus* (RnCOX19, XM_221972), *Mus musculus* (MmCOX19, NM_197980), *Homo sapiens* (HsCOX19, AY957566), *Arabidopsis thaliana* (AtCOX19-1.1, At1g66590.1; AtCOX19-1.2, At1g66590.2), *Oryza sativa* (OsCOX19, AK120143), *Zea mays* (ZmCOX19, BI675181), *Triticum aestivum* (TaCOX19, BQ579224), *Glycine max* (GmCOX19, BE658914), *Saccharomyces cerevisiae* (ScCOX19, Z73123) and *Schizosaccharomyces pombe* (SpCOX19, NM_001022867)

Comparison of the deduced protein sequences from *AtCOX19* genes and homologues from non-plant species indicates the presence of conserved residues in the central portion of the protein and somewhat more variable regions in the N- and C-terminal portions (Fig. 1B). Four cysteine residues conserved in all COX19 proteins, forming two Cx_9C motifs, are also present in AtCOX19. It has been recently shown that cysteines in these motifs, also observed in the copper chaperone COX17, participate in copper binding (Rigby et al. 2007). In addition, these motifs participate in the transport of COX19 proteins to mitochondria by the Mia40 import pathway (Mesecke et al. 2005). Within the plant kingdom, cDNA sequences encoding putative COX19 homologues were found in several species (Fig. 1B). The plant proteins have highly conserved N-terminal portions but differ at the C-terminus. COX19 from monocots contain a short C-terminal extension. The only protein with a significant difference at the N-terminus is the one encoded by the *AtCOX19-1.2* splice variant. This form may have arisen from particular characteristics of the Arabidopsis *COX19-1* gene and seems to have no counterparts in other plants. As for yeast Cox19p, none of the Arabidopsis COX19 forms is predicted to be located into mitochondria with the only exception of COX19-1.2, which is predicted to be mitochondrial with a probability of 0.7 only when using the program MitoProt.

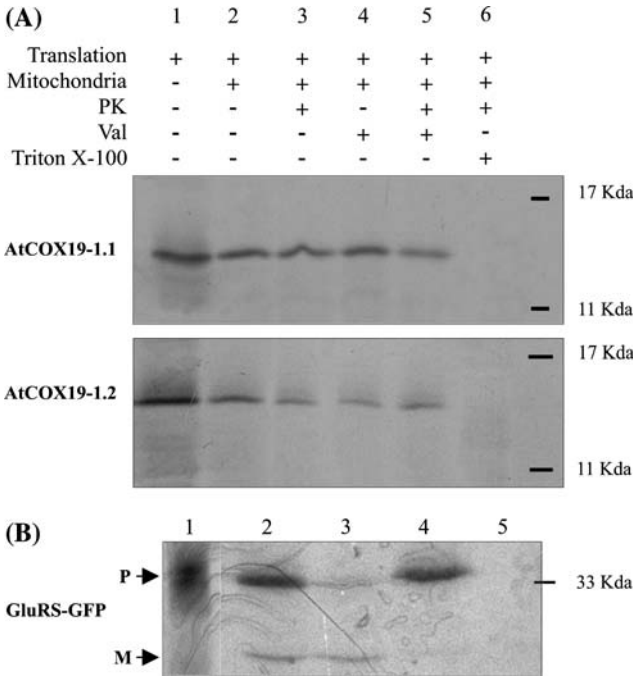

Fig. 2 Import of AtCOX19 isoforms (**A**) and preGluRS-GFP (**B**) into plant mitochondria. One microliter of the translation product was loaded in lane 1. Import assays were performed with 50 µg of potato mitochondria and 5 µl of translation product (lanes 2–6). Mitochondria were treated with valinomycin (Val) prior to import (lanes 4 and 5). After import, mitochondria were subjected to Triton X-100 (lane 6) and treated with proteinase K (PK; lanes 3, 5, and 6). The precursor (P) and mature (M) forms of GluRS-GFP are indicated in B

Both AtCOX19 proteins are imported to plant mitochondria and are bound to the intermembrane space side of the inner membrane

We performed in vitro import assays to determine whether AtCOX19 proteins are mitochondrial. When AtCOX19-1.1 and AtCOX19-1.2 are translated in vitro, products with apparent molecular weight of 13 and 15 kDa, which fit the calculated sizes (10.9 and 12.7 kDa, respectively) are obtained (Fig. 2A, lane 1). After import, no processed band appears (Fig. 2A, lane 2) but both translation products are resistant to proteinase K (Fig. 2A, lane 3). This protection is lost when the mitochondrial membranes are solubilized by Triton X-100 before proteinase K treatment (Fig. 2A, lane 6) indicating that the protection is due to the membrane and not to protease resistance of the protein. These data indicate that both proteins are imported into mitochondria without apparent processing. Similar results were obtained using potato and Arabidopsis mitochondria. The import of COX19 is not inhibited by the ionophore valinomycin indicating that an electrical membrane potential is not required (Fig. 2A, lane 5). Positive controls of import experiments were done with the GluRS targeting sequence fused to GFP (Duchêne et al. 2005). This protein, imported into mitochondria and processed in a membrane potential dependent manner, was used in order to validate the competence of mitochondria for import and the efficiency of proteinase K and valinomycin treatments (Fig. 2B). The 33.8 kDa precursor protein is processed into a 28.0 kDa protease resistant protein. Import is strongly inhibited by valinomycin treatment indicating, in this case, the requirement of a membrane potential for import. Proteinase K treatment is efficient to degrade protein that was not imported (Fig. 2B, compare lanes 4 and 5). The residual precursor signal in lane 3 corresponds to imported protein not yet processed.

The location of AtCOX19 after import was analyzed. Mitochondria treated with proteinase K after the import assay were separated into soluble and membrane protein fractions. In absence of salt and detergent, both AtCOX19 isoforms were present in the membrane fraction (Fig. 3A). The quality of the fractionation was tested by Western blot with the same protein fractions using antibodies directed against the soluble MnSOD and the membrane CCMH protein as controls. When mitochondria were swollen after import and treated with proteinase K the signal of the imported proteins disappeared indicating that COX19 proteins were accessible to proteinase K. This treatment produced the complete disappearance of CCMH, a protein

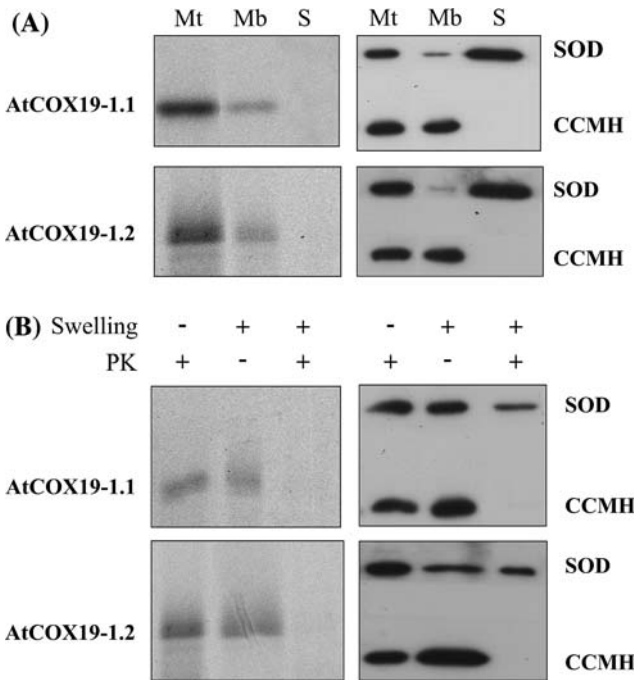

Fig. 3 Submitochondrial localization of imported AtCOX19. Import assays were performed as described in Fig. 2. (**A**) After import, mitochondria (Mt) were broken by three freeze/thaw cycles and membrane (Mb) and soluble (S) fractions were obtained. (**B**) Mitochondria were swollen after import to disrupt the outer membrane as described in Materials and methods. Intact or swollen mitochondria were treated with proteinase K (PK). All assays were divided in two and analyzed by autoradiography (left part) and by Western blots (right part). Antibodies against the soluble matrix protein superoxide dismutase (SOD) and against CCMH, an inner membrane protein oriented towards the intermembrane space, were used as control

attached to the inner membrane and facing the intermembrane space (Meyer et al. 2005), but not that of the matrix MnSOD, indicating that the outer membrane was disrupted but the inner membrane was largely intact (Fig. 3B).

We conclude that AtCOX19 is imported into mitochondria by a process that does not require a membrane potential or a cleavable presequence. Once imported, AtCOX19 remains bound to the intermembrane space side of the inner membrane. This conclusion is valid for both AtCOX19 isoforms.

Complementation of a yeast *cox19* mutant by one of the AtCOX19 isoforms

Information about the functionality of the putative AtCOX19 proteins was obtained by complementation analysis of a yeast *cox19* mutant. This mutant has a defect in respiration and is then unable to grow on non-fermentable carbon sources such as ethanol, while it grows on media containing glucose (Nobrega et al. 2002). To test

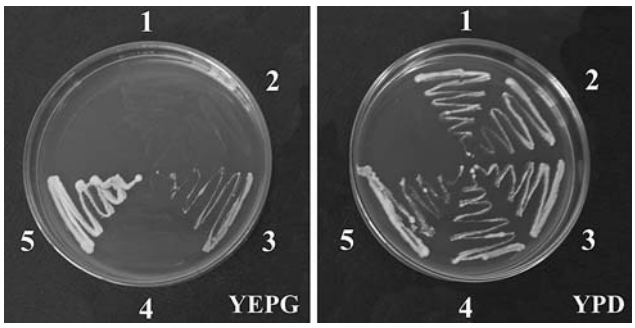

Fig. 4 Complementation of a *cox19* yeast mutant by AtCOX19-1.1. A *cox19* null yeast mutant strain transformed with either empty expression plasmid pYPGE15 (2) or the same plasmid carrying the AtCOX19-1.1 coding region in the sense (3) or antisense (4) orientation was streaked in media containing fermentable (YPD) or non-fermentable (YEPG) carbon sources. As additional controls, non-transformed mutant (1) and wild-type (5) strains were used

if the products of the *AtCOX19* genes are functional in yeast, we have cloned cDNAs from both *AtCOX19-1* splice variants in the sense and antisense orientations in plasmid pYPGE15 (Brunelli and Pall 1993), containing a constitutive phosphoglycerate kinase (*PGK*) gene promoter and a *CYC1* terminator. Introduction of a plasmid containing *AtCOX19-1* variant 1 in the sense orientation into a *cox19* mutant yeast strain produced cells able to grow on both fermentable and non-fermentable carbon sources (Fig. 4). Cells transformed with the pYPGE15 plasmid either without insert or with the insert in the reverse orientation were unable to grow on non-fermentable medium. This result indicates that AtCOX19-1.1 is able to functionally replace yeast Cox19p in the COX biogenesis pathway, suggesting that AtCOX19-1.1 is indeed the functional homologue of the yeast protein. This also applies to the protein encoded by *AtCOX19-2*, since it is identical to AtCOX19-1.1. Conversely, when a similar experiment was conducted with a cDNA corresponding to splice variant 2, no complementation was observed (not shown).

Expression of *AtCOX19* genes

Northern experiments using total RNA extracted from different organs of mature plants showed that *AtCOX19* transcripts are present at similar levels in all organs tested (Fig. 5, upper panel). We have analyzed the relative levels of both *AtCOX19* splice variants in different organs by performing competitive RT-PCR using primers that amplify both forms but produce fragments of different size. Variant 1 is much more abundant under all conditions tested, since variant 2 could not be detected in these experiments (not shown). We were unable to discern if the PCR product corresponding to variant 1 was derived from *AtCOX19-1* or *AtCOX19-2*, since both transcripts are

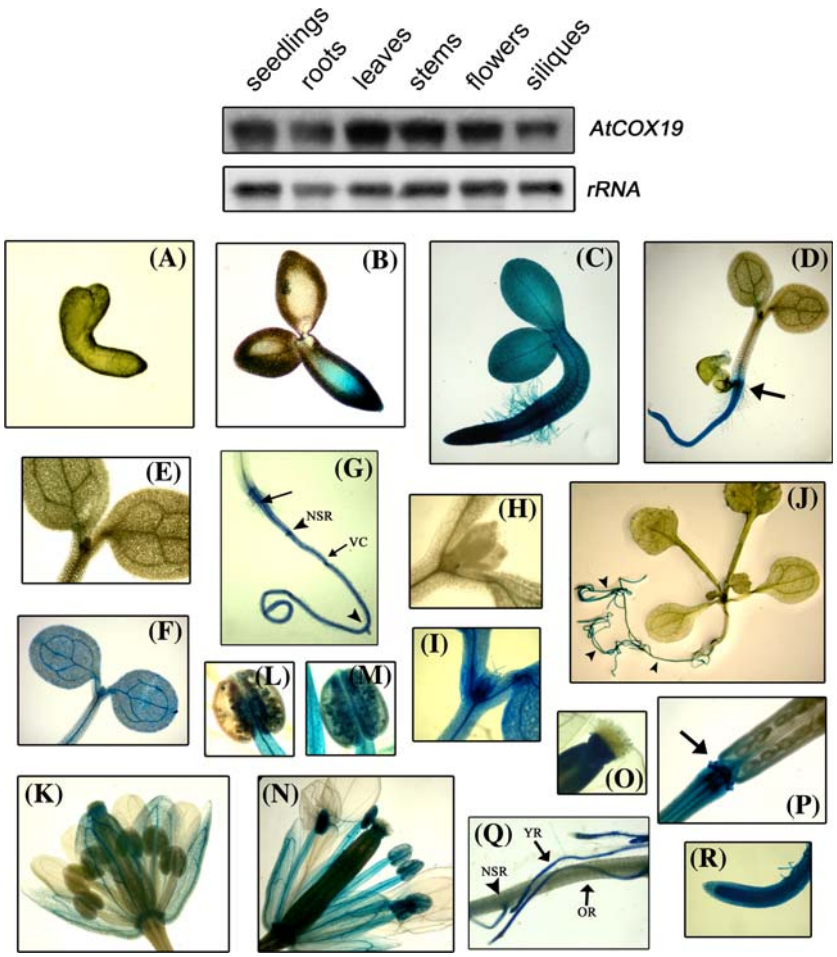

Fig. 5 Expression of *AtCOX19* genes in different organs. A northern blot using total RNA (15 μg) extracted from different organs of 4-week Arabidopsis plants and hybridized with a full-length probe for the *AtCOX19-1* gene is shown in the upper panel. Hybridization to an rRNA probe is also shown for reference. (**A–R**) Histochemical localization of GUS activity in Arabidopsis plants transformed with the *AtCOX19-1* region located upstream of exon 2 fused to the *gus* reporter gene. (**A**) Embryo in late torpedo stage. (**B–J**) One- (**B**), two- (**C**), three- (**D**), four- (**E–G**), six- (**H, I**), or 13-day-old seedlings (**J**) were incubated in the presence of the chromogenic substrate during 1.5 h (**A, B, D, E, G, H, J**) or overnight (**C, F, I**) as described in Materials and methods. Flowers (**K, N**) and roots (**Q, R**) from adult plants were also analyzed. (**L, M**) Details of anthers from K and N, respectively. (**O, P**) Stigma and receptacle. NSR, nascent secondary root; VC, vascular cylinder; OR and YR, older and younger root, respectively

nearly identical. The frequency of cDNA annotations from each of these genes in data banks suggests, however, that *AtCOX19-1* is expressed at higher or similar levels than *AtCOX19-2*. As a consequence, we conclude that a considerable amount of the PCR product originates from splice variant 1 of *AtCOX19-1* and that this form is much more abundant than splice variant 2, at least within the tissues tested. Transcripts corresponding to splice variant 2 were only detected when using primers specific for this form.

The expression characteristics of *AtCOX19* genes were also analyzed by producing plants bearing *AtCOX19-1* non-transcribed upstream regions plus transcribed sequences down to exon 2 nucleotide 26 translationally fused to the *gus* coding region (Fig. 1A). Seedlings grown in Petri dishes on Murashige and Skoog medium showed strong staining in roots (Fig. 5, B–D, G, and J). Activity in roots was already evident at very early stages of development (1–2 days after imbibition), but not in embryos at late stages of embryogenesis (Fig. 5A), and was higher in the root meristem, the vascular cylinder and nascent secondary roots. If incubation with the reagent was prolonged overnight, staining was also observed in hypocotyls and cotyledons, mainly in the vascular tissues, and in leaf primordia (Fig. 5, C, F, and I). Adult plants grown on soil displayed activity in roots, flowers and siliques, but not in leaves and stems (Fig. 5, K–R). Expression patterns in roots changed upon development. In young root tissues, GUS activity was particularly evident in root tips, the vascular cylinder and nascent secondary roots, while in older roots no staining was observed (Fig. 5, Q and R). In flowers, expression was detected in petal veins and in anther filaments (Fig. 5, K–N). Expression in pollen was only evident after anthesis (Fig. 5, L and M). Staining was also detected in the receptacle of flowers and siliques (Fig. 5, K and P). We have not made constructs using the *AtCOX19-2* upstream region. We speculate, however, that the expression pattern of *AtCOX19-2* must be very similar to that of *AtCOX19-1*, since both genes share almost 100% identity in the region located 430 bp upstream of the start codon and since deletion of the *AtCOX19-1* region located upstream of –430 does not produce noticeable changes in expression (not shown).

AtCOX19 expression is induced by metals

In view of a possible role of AtCOX19 in metal transport, we have tested the effect of incubation of plants in solutions containing copper, zinc and iron salts on *AtCOX19* expression. As observed in Fig. 6A, $CuSO_4$ (50 μM and 5 mM) produced an increase in *AtCOX19* transcript levels after 8 h of incubation. Incubation in the presence of zinc and iron also induced *AtCOX19* expression (Fig. 6A).

The effect of different copper concentrations on the transcriptional activity of the *AtCOX19-1* promoter was assayed by infiltration of leaves with the corresponding solutions. As shown in Fig. 6B, a significant increase in expression was observed with 10 μM $CuSO_4$, while higher concentrations were less effective. The effect of copper was also observed when plants grown in vermiculite were irrigated with $CuSO_4$ solutions during two days (Fig. 6B). As in northern experiments, zinc and iron also produced an increase in expression of the reporter gene.

AtCOX19 is induced by biotic and abiotic stress factors

Histochemical analysis of GUS expression in leaves and stems of plants transformed with the *AtCOX19-1* promoter-*gus* fusion showed a localized expression in regions where cuts were produced to separate these organs from plants suggesting that *AtCOX19-1* may be induced by wounding. Accordingly, we wounded leaves and stems in several ways and analyzed GUS activity by the histochemical method after incubating them for 2 h. A localized increase in GUS activity was observed in regions adjacent to damaged zones (Fig. 7, A, B, D, and G–J), indicating that wounding induces *AtCOX19-1* promoter-dependent expression. To exclude the possibility that the localized increase in staining was due to better accessibility of the dye to the damaged regions, we performed similar experiments with plants transformed with the *gus* gene fused to different promoters, including Arabidopsis *Cytc-2* (Welchen and Gonzalez 2005) and *COX5c-2* (Curi et al. 2005). No induction was observed in wounded organs from these plants (Fig. 7, C and E), suggesting that the observed effect is indeed dependent on the *AtCOX19-1* promoter. In addition, a localized increase in GUS expression was observed in senescent leaves (Fig. 7K). It should be mentioned that both splice variants would produce GUS activity from this construct, since it comprises sequences down to exon 2. The observed expression pattern represents, then, the sum of both transcript forms.

Induction of the *AtCOX19-1* promoter by wounding was quantified by measuring GUS specific activity in leaf protein extracts. As shown in Fig. 7N, a two to threefold increase in GUS activity was observed shortly after wounding (1–6 h), indicating the existence of a direct response to cell or tissue damage. The effect of wounding on *AtCOX19* gene expression was also observed by northern analysis of *AtCOX19* transcript levels in leaves of non-transformed plants (not shown).

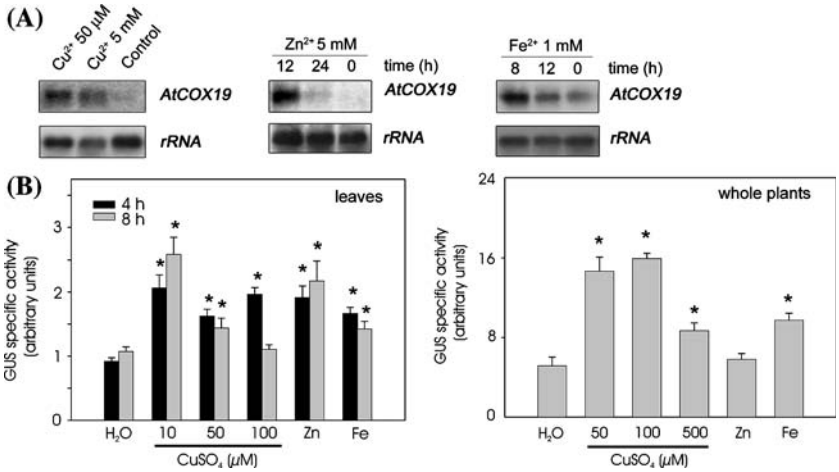

Fig. 6 Induction of *AtCOX19* genes by metals. (**A**) Arabidopsis plants were incubated during 8 h in solutions containing either 50 μM or 5 mM $CuSO_4$, as indicated. After incubation, total RNA was extracted and analyzed in a northern experiment with an *AtCOX19-1* probe as described in Materials and methods. Plants incubated for different times in the presence of either 5 mM $ZnCl_2$ or 1 mM $FeSO_4$ were analyzed in a similar way. Hybridization to an rRNA probe is also shown for reference. (**B**) GUS activity was measured using the fluorogenic substrate MUG and protein extracts prepared at different times after treatment of plants transformed with the *AtCOX19-1::gus* fusion. Leaves were infiltrated with either H_2O, $CuSO_4$ at different concentrations, 1 mM $ZnCl_2$, or 1 mM $FeSO_4$. Whole plants were grown in vermiculite during 10 days and then irrigated during two additional days with solutions containing either $CuSO_4$ at different concentrations, 1 mM $ZnCl_2$, or 1 mM $FeSO_4$. Pools of 5 independent lines were used for the analysis. Error bars represent SD of three independent activity measurements. Asterisks indicate significant changes in expression respective to controls ($P < 0.05$) as indicated by *t*-tests

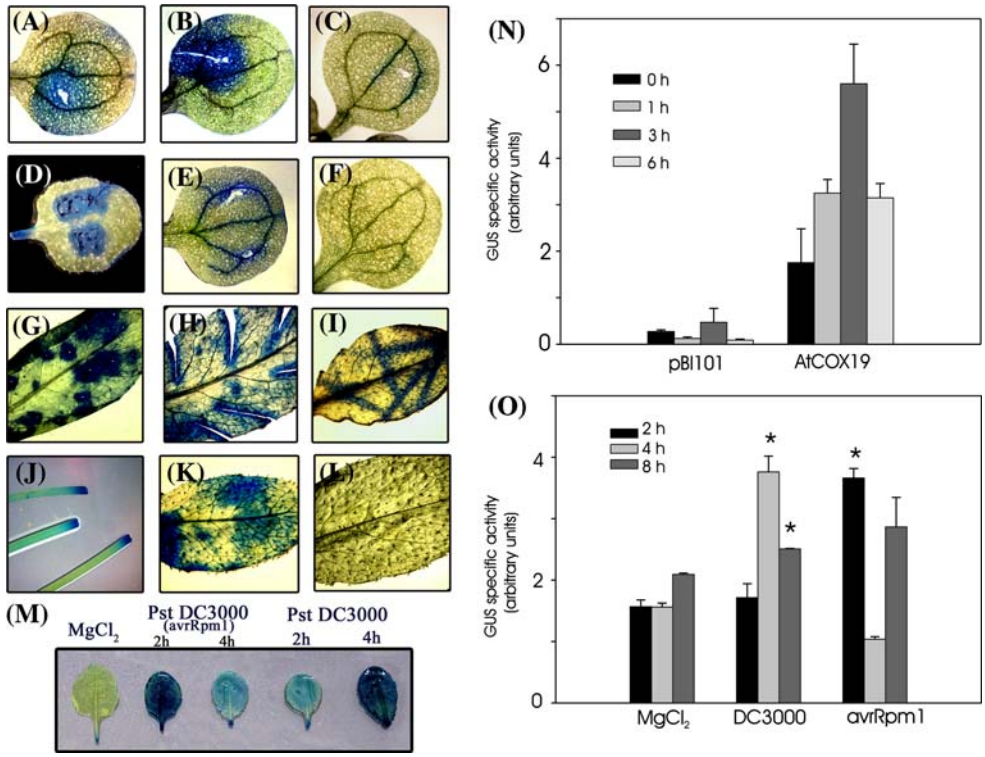

Fig. 7 Induction of *AtCOX19-1* by wounding and pathogens. (**A–M**) Histochemical analysis of *AtCOX19-1* expression. Organs from plants transformed with the *AtCOX19-1* upstream region fused to *gus* were wounded in different ways, either drilled (**A, D, G**), cut (**B, H, J**), or folded (**I**), 2 h before the histochemical assay of GUS expression was performed. Plants transformed with *AtCytc-2* (**C**) or *AtCOX5c-2* (**E**) promoter-*gus* fusions were treated in a similar way. (**F, L**) Control untreated leaves. (**K**) Senescent leaf of a plant transformed with the *AtCOX19-1* promoter/*gus* fusion. (**M**) Histochemical detection of GUS activity in leaves infiltrated with suspensions of the pathogenic bacterium *Pseudomonas syringae* pv. tomato (Pst DC3000, virulent strain; Pst DC3000 (avrRpm1), avirulent strain). Leaves were immersed in the GUS staining solution 2 or 4 h after infiltration and incubated 2 h at 37°C. A solution of 1 mM $MgCl_2$ was used as a mock control of infiltration. (**N, O**) GUS activity was measured in leaves of plants transformed with *AtCOX19-1* gene regions fused to *gus* at different times after wounding (**N**) or exposure to virulent (DC3000) or avirulent (avrRpm1) *Pseudomonas syringae* pv. tomato strains (**O**). Plants transformed with a promoterless *gus* gene (pBI101) were used as control in (**N**). A solution of 1 mM $MgCl_2$ was used as a mock control of infiltration in (**O**). Measurements were performed on a pool of five independent lines. Error bars represent SD of three independent activity measurements. Asterisks indicate significant changes in expression respective to controls ($P < 0.05$) as indicated by *t*-tests

Inoculation of leaves with virulent and avirulent strains of the pathogen *Pseudomonas syringae* pv. tomato also produced an increase in the transcriptional activity of the *AtCOX19-1* promoter when analyzed by both histochemical (Fig. 7M) and fluorometric methods (Fig. 7O). Induction was observed earlier with the avirulent strain, suggesting that *AtCOX19* expression may be closely associated with the induction of the hypersensitive response.

Considering that the response to wounding and pathogens may arise from oxidative stress originated by these treatments (Orozco-Cardenas and Ryan 1999), we have tested the effect on expression of salicylic acid, a compound that produces an increase in reactive oxygen species and acts as a mediator of the response to pathogens (Rao et al. 1997). We also analyzed the effect of the nitric oxide donor SNP, since this compound acts as a mediator of some stress responses (Grun et al. 2006). Northern analysis of *AtCOX19* transcript levels indicated that salicylic acid treatment produced a slight and transient increase in transcript levels after a few hours of incubation (Fig. 8A). SNP, in turn, produced a much higher effect on expression. A several fold increase in *AtCOX19* expression was evident after 4 h of treatment, but transcript levels returned to normal values after higher incubation times (Fig. 8A). A similar effect of the compounds tested was observed when measuring GUS activity of plants transformed with *AtCOX19-1* promoter/*gus* fusions (Fig. 8, B–D). In these plants, we also assayed the effect of 3-AT, another compound that produces an increase in reactive oxygen species (Wang et al. 1999). GUS activity levels in extracts of leaves infiltrated with 3-AT were considerably higher than those observed in leaves that were infiltrated with MS as control (Fig. 8, B and E).

We have also analyzed the expression of *AtCOX19* genes using RT-PCR. During the RT-PCR experiments we

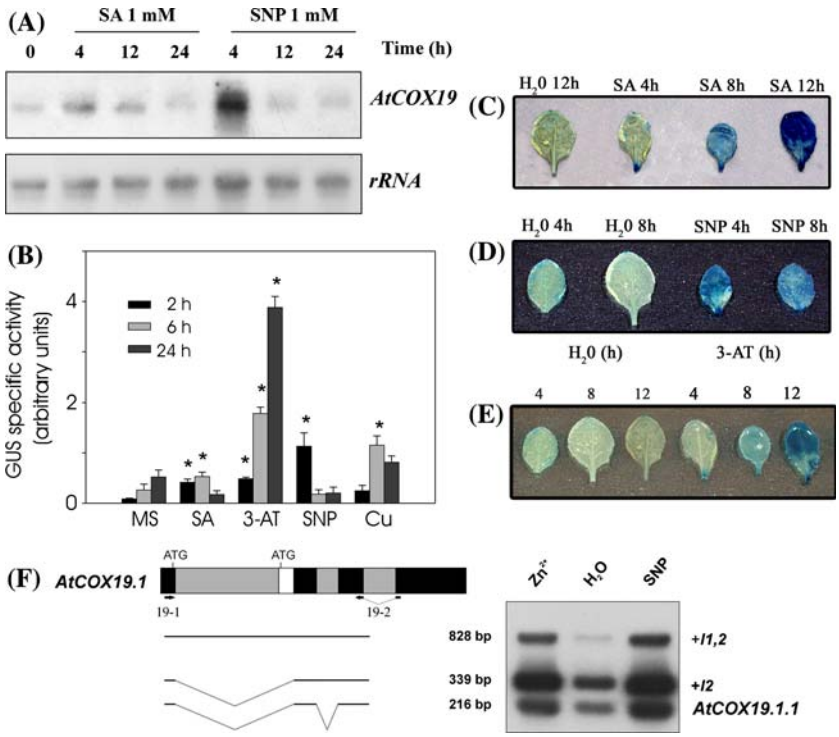

Fig. 8 Effect of compounds that produce oxidative stress on the expression of *AtCOX19* genes. (**A**) Arabidopsis plants were incubated in solutions containing salicylic acid (SA) or sodium nitroprusside (SNP). After different incubation times, total RNA was extracted and analyzed in a northern experiment with an *AtCOX19-1* probe as described in Materials and methods. Hybridization to an rRNA probe is also shown for reference. (**B**) GUS activity was measured in leaves of plants transformed with *AtCOX19-1* gene regions fused to *gus* at different times after treatment with salicylic acid (SA), sodium nitroprusside (SNP), 3-AT, or 10 μM $CuSO_4$. Plants incubated with Murashige and Skoog medium (MS) were used as control. Measurements were performed on a pool of five independent lines. Error bars represent SD of three independent activity measurements. Asterisks indicate significant changes in expression respective to controls ($P < 0.05$) as indicated by *t*-tests. (**C–E**) Histochemical analysis of GUS expression after treatment of leaves with salicylic acid (SA, panel **C**), sodium nitroprusside (SNP, panel **D**), or 3-AT (panel **E**) incubated for different times, as indicated, before immersing them in the GUS staining solution. Color development was stopped when satisfactory staining was obtained with each of the reagents. All samples shown in each panel were stained during the same time (**F**) RT-PCR analysis of transcripts from untreated plants, or plants incubated in the presence of 5 mM $ZnCl_2$ or 1 mM SNP for 12 or 4 h, respectively. A hybridization of products obtained after 25 rounds of amplification (within the linear range) is shown. A scheme showing the *AtCOX19* regions represented by the different products, together with the positions of the primers used for amplification (19-1 and 19-2), is shown to the left. The bands representing the spliced transcript (*mature*) and forms with intron 2 (*+I2*) and 1 + 2 (*+I1 + I2*) are indicated

noted the presence of bands of higher molecular weight than those expected for the cDNAs (Fig. 8F). These bands were not unspecific amplification products, since they hybridized with an *AtCOX19* probe. The most prominent product migrated as a 306 bp DNA fragment when using oligonucleotides that hybridize at the 3′ end of exons 1 and 3. Accordingly, we speculate that it arises from a partially unspliced transcript in which intron 1 was removed but intron 2 was still present. Another band of 766 bp was also observed, arising from transcripts with introns 1 and 2 (Fig. 8F). This suggests that stable *AtCOX19* unspliced transcripts are present in Arabidopsis. In fact, we have noted the presence of two ESTs that represent transcripts with unspliced introns 2 or 3 (accession numbers BT015476 and CF651618, respectively). Due to the presence of unspliced transcripts, we also considered the possibility of a post-transcriptional regulation of splicing efficiency. So far, we were unable to detect significant variations in the relative abundance of the different transcript forms in samples obtained from plants subjected to different treatments that induce *AtCOX19* expression (Fig. 8F and results not shown).

As a general conclusion, it was observed that *AtCOX19* gene(s) are induced by several factors that produce stress and an increase in reactive oxygen species. Indeed, the response to metals described above may also be caused by an increase in reactive oxygen species originated by these compounds. These responses may be related with a higher demand on AtCOX19 protein levels to replace inactivated or damaged COX or isolated subunits.

Discussion

Since free copper and zinc are toxic to the cell when present in excess, they are usually stored and mobilized bound to specific proteins (Wintz et al. 2001). In addition, certain proteins known as metallochaperones participate in the delivery of metal ions to specific cell compartments or proteins (Harrison et al. 1999; Rosenzweig 2002; Pilon et al. 2006). In this study, we report the identification of AtCOX19, a functional homologue of Cox19p from yeast, putatively involved in the delivery of metal(s) from an unknown source to COX, either directly or through an intermediate protein (Nobrega et al. 2002; Rigby et al. 2007). We demonstrate that AtCOX19 is a mitochondrial protein able to rescue the respiration-deficient phenotype of a yeast *cox19* null mutant. The fact that AtCOX19 is functional in the heterologous system suggests that the entire pathway is conserved between yeast and plants.

In vitro experiments demonstrated that AtCOX19 is imported into mitochondria. Both isoforms are attached to the inner membrane and orientated towards the intermembrane space, which is consistent with the fact that the membrane potential is not necessary for the import process. In yeast, COX19 is imported into the mitochondrial intermembrane space by a disulfide relay system described recently (Mesecke et al. 2005; Rissler et al. 2005). Rather than an N-terminal presequence, characteristic cysteine motifs are involved in this import pathway. AtCOX19, as its yeast ortholog, presents conserved twin Cx_9C motifs. Although the existence of this system has not been demonstrated in plants, we tried to affect AtCOX19 import by treatment with reducing agents, as observed in yeast (Mesecke et al. 2005). We could not inhibit AtCOX19 import by treating mitochondria with 20 mM DTT prior to import (data not shown).

AtCOX19-1 undergoes alternative splicing. One of the transcript forms encodes a protein with an N-terminal extension compared with COX19 proteins from other organisms. This protein, unlike the shorter form, was unable to complement a yeast *cox19* mutant. This may either indicate that this isoform is not functional, that it is not imported into mitochondria or that it is not efficiently expressed in yeast. This last possibility seems unlikely since the same promoter was used and the ATG contexts of both variants were modified to be identical (TAC-AAAGATGA). It is also unlikely that targeting to mitochondria of variant 2 is affected in yeast, since it was imported into Arabidopsis mitochondria. The most likely explanation is that AtCOX19-1.2 is not functional in yeast. In this sense, it is the only COX19 protein with a significant N-terminal extension. Whether AtCOX19-1.2 fulfils a function in Arabidopsis is unknown.

It is noteworthy that incompletely spliced transcripts arising from *AtCOX19* genes were detected in total RNA. In Arabidopsis, an unusually high proportion of genes (2–3%) produce stable transcripts with retained introns which may have a regulatory function (Iida et al. 2004; Ner-Gaon et al. 2004). So far, we have not detected changes in the relative abundance of the different transcript forms as a consequence of treatments that induce *AtCOX19* expression.

The postulated function of COX19, related to intracellular metal transport for COX assembly, would suggest that this protein is required in tissues or cells with active mitochondrial biogenesis. Expression in anthers and root meristems may be related to this, since mitochondrial number per cell is higher in these tissues (Lee and Warmke 1979; Fujie et al. 1993). Accordingly, the promoters of several genes encoding respiratory chain components direct expression of reporter genes in the same tissues (Zabaleta et al. 1998; Elorza et al. 2004; Welchen et al. 2004; Curi et al. 2005; Welchen and Gonzalez 2005).

Localization experiments in yeast indicated that Cox19p is present in both the cytosol and the mitochondrial intermembrane space (Nobrega et al. 2002). Recent studies suggested that only the mitochondrial location is necessary for COX assembly since respiratory function is active when COX19 is tethered to the inner membrane (Rigby et al. 2007). If not necessary for COX biogenesis, the existence of a cytosolic form raises the possibility of additional roles for COX19. Analysis of COX19 expression patterns in a pluricellular organism such as Arabidopsis might shed light on these possible functions. Indeed, the strong expression in young roots may be an indication of a more general role of AtCOX19 as a chaperone in the transport of metals, which are incorporated through roots.

The steady-state amount of *AtCOX19* transcripts is increased upon incubation of plants in solutions containing copper. Although this response may reflect a role of AtCOX19 in the transport of this metal, it can also be proposed that *AtCOX19* expression responds to damage produced by accumulation of high levels of copper, perhaps through an increase in reactive oxygen species (Drazkiewicz et al. 2004). Accordingly, *AtCOX19* was also induced by treatment of plants with agents involved in the production of reactive oxygen species, including 3-AT, SNP and salicylic acid and by pathogen infection and wounding of leaves. It is well known that different types of stress induce the alternative pathway of respiration (Møller 2001). This induction is part of a response to lower the generation of reactive oxygen species under conditions that limit the electron flow through the cytochrome pathway. Our results suggest that, in addition to increasing the capacity of alternative respiration, plant cells induce proteins involved in the biogenesis of the cytochrome

pathway, presumably to replace inactive components. In this sense, it has been observed that genes encoding another metallochaperone involved in COX assembly, AtCOX17, show very similar responses to stress factors (Balandin and Castresana 2002; Attallah et al. 2007). In addition, the analysis of publicly available microarray data indicates that genes encoding homologues of other COX assembly factors, such as COX15 and SCO1, and a group of plant-specific COX subunits (COXX1, COXX6; Millar et al. 2004) are also induced by pathogens and other stress factors. This response is not observed for a majority of genes encoding COX subunits, perhaps reflecting the fact that assembly factors but not structural components are limiting under stress conditions. Whether *AtCOX19* gene expression is induced by reactive oxygen species or damage produced within the mitochondrion (a sort of retrograde regulation) or elsewhere in the cell is not clear from our results. In support of the existence of a mitochondrial signal for expression, induction of *AtCOX19* by rotenone, an inhibitor of the electron transport chain at the level of Complex I, has been observed in microarray experiments (Lister et al. 2004).

Considering its expression characteristics, it cannot be ruled out that AtCOX19 has additional functions besides its participation in COX assembly as, for example, metal transport, detoxification, or general protection against oxidative stress. Further studies will be oriented to dissect the signal transduction pathway that operates in *AtCOX19* induction and to isolate mutants in the corresponding genes to analyze in detail the role of this protein in plants.

Acknowledgments We thank Alexander Tzagoloff (Columbia University, New York) for sending us yeast strains and Malena Alvarez (CIQUIBIC, Universidad Nacional de Córdoba, Argentina) for providing us the *Pseudomonas syringae* strains. We also thank the RIKEN BRC Experimental Plant Division (Japan) for sending us full-length cDNA clones. This work was supported by grants from CONICET, ANPCyT (Agencia Nacional de Promoción Científica y Tecnológica), Universidad Nacional del Litoral and by the Centre National de la Recherche Scientifique. Travel grants were obtained from the SECYT-ECOS project A03B04. CVA is a fellow of CONICET (Argentina); EW and DHG are members of the same Institution. CP is supported by a grant from the French Ministère délégué à l'Enseignement Supérieur et à la Recherche.

References

Alvarez ME, Pennell RI, Meijer PJ, Ishikawa A, Dixon RA, Lamb C (1998) Reactive oxygen intermediates mediate a systemic signal network in the establishment of plant immunity. Cell 92: 773–784

Attallah CV, Welchen E, Gonzalez DH (2007) The promoters of *Arabidopsis thaliana* genes *AtCOX17-1* and *-2*, encoding a copper chaperone involved in cytochrome *c* oxidase biogenesis, are preferentially active in roots and anthers and induced by biotic and abiotic stress. Physiol Plant 1290:123–134

Baker KE, Parker R (2004) Nonsense-mediated mRNA decay: terminating erroneous gene expression. Curr Opin Cell Biol 16:293–299

Balandin T, Castresana C (2002) AtCOX17, an Arabidopsis homolog of the yeast copper chaperone COX17. Plant Physiol 129: 1852–1857

Barrientos A, Barrios MH, Valnot I, Rötig A, Rustin P, Tzagoloff A (2002) Cytochrome oxidase in health and disease. Gene 286:53–63

Brunelli JP, Pall ML (1993) A series of yeast shuttle vectors for expression of cDNAs and other DNA sequences. Yeast 9: 1299–1308

Capaldi RA (1990) Structure and function of cytochrome *c* oxidase. Annu Rev Biochem 59:569–596

Carpenter CD, Simon AE (1998) Preparation of RNA. In: Martinez-Zapater J, Salinas J (eds) Methods in molecular biology, vol. 82. Arabidopsis protocols. Humana Press Inc, Totowa, NJ, pp 85–89

Clough SJ, Bent AF (1998) Floral dip: a simplified method for *Agrobacterium*-mediated transformation of *Arabidopsis thaliana*. Plant J 16:735–743

Cobine PA, Pierrel F, Winge DR (2006) Copper trafficking to the mitochondrion and assembly of copper metalloenzymes. Biochim Biophys Acta 1763:759–772

Curi GC, Chan RL, Gonzalez DH (2005) The leader intron of *Arabidopsis thaliana* genes encoding cytochrome c oxidase subunit 5c promotes high-level expression by increasing transcript abundance and translation efficiency. J Exp Bot 56: 2563–2571

Curi GC, Welchen E, Chan RL, Gonzalez DH (2003) Nuclear and mitochondrial genes encoding cytochrome *c* oxidase subunits respond differently to the same metabolic factors. Plant Physiol Biochem 41:689–693

Diekert K, de Kroon AI, Ahting U, Niggemeyer B, Neupert W, de Kruijff B, Lill R (2001) Apocytochrome *c* requires the TOM complex for translocation across the mitochondrial outer membrane. EMBO J 20:5626–5635

Drazkiewicz M, Skorzynska-Polit E, Krupa Z (2004) Copper-induced oxidative stress and antioxidant defence in *Arabidopsis thaliana*. Biometals 17:379–387

Duchêne AM, Giritch A, Hoffmann B, Cognat V, Lancelin D, Peeters NM, Zaepfel M, Marechal-Drouard L, Small ID (2005) Dual targeting is the rule for organellar aminoacyl-tRNA synthetases in *Arabidopsis thaliana*. Proc Natl Acad Sci USA 102: 16484–16489

Duchêne AM, Peeters N, Dietrich A, Cosset A, Small ID, Wintz H (2001) Overlapping destinations for two dual targeted glycyl-tRNA synthetases in *Arabidopsis thaliana* and *Phaseolus vulgaris*. J Biol Chem 276:15275–15283

Elorza A, León G, Gómez I, Mouras A, Holuigue L, Araya A, Jordana X (2004) Nuclear *SDH2-1* and *SDH2-2* genes, encoding the iron-sulfur subunit of mitochondrial complex II in Arabidopsis, have distinct cell-specific expression patterns and promoter activities. Plant Physiol 136:4072–4087

Fujie M, Kuroiwa H, Kawano S, Kuroiwa T (1993) Studies on the behavior of organelles and their nucleoids in the root apical meristem of *Arabidopsis thaliana* (L.) Col. Planta 189:443–452

Glerum DM, Shtanko A, Tzagoloff A (1996) Characterization of COX17, a yeast gene involved in copper metabolism and assembly of cytochrome oxidase. J Biol Chem 271: 14504–14509

Grun S, Lindermayr C, Sell S, Durner J (2006) Nitric oxide and gene regulation in plants. J Exp Bot 57:507–516

Harrison MD, Jones CE, Dameron CT (1999) Copper chaperones: function, structure and copper-binding properties. J Biol Inorg Chem 4:145–153

Herrmann JM, Funes S (2005) Biogenesis of cytochrome oxidase—sophisticated assembly lines in the mitochondrial inner membrane. Gene 354:43–52

Hull GA, Devic M (1995) The beta-glucuronidase (gus) reporter gene system. Gene fusions; spectrophotometric, fluorometric, and histochemical detection. In: Jones H (ed) Methods in plant molecular biology, vol 49: plant gene transfer and expression protocols. Humana Press Inc, Totowa, NJ, pp 125–141

Iida K, Seki M, Sakurai T, Satou M, Akiyama K, Toyoda T, Konagaya A, Shinozaki K (2004) Genome-wide analysis of alternative pre-mRNA splicing in *Arabidopsis thaliana* based on full-length cDNA sequences. Nucleic Acids Res 32: 5096–5103

Jefferson RA, Kavanagh TA, Bevan MW (1987) GUS fusions: *β*-glucuronidase as a sensitive and versatile gene fusion marker in higher plants. EMBO J 20:3901–3907

Khalimonchuk O, Rödel G (2005) Biogenesis of cytochrome *c* oxidase. Mitochondrion 5:363–388

Lee SLJ, Warmke HE (1979) Organelle size and number in fertile and T-cytoplasmic male-sterile corn. Am J Bot 60:141–148

Lister R, Chew O, Lee MN, Heazlewood JL, Clifton R, Parker KL, Millar AH, Whelan J (2004) A transcriptomic and proteomic characterization of the Arabidopsis mitochondrial protein import apparatus and its response to mitochondrial dysfunction. Plant Physiol 134:777–789

Mesecke N, Terziyska N, Kozany C, Baumann F, Neupert W, Hell K, Herrmann J (2005) A disulfide relay system in the intermembrane space of mitochondria that mediates protein import. Cell 121:1059–1069

Meyer EH, Giegé P, Gelhaye E, Rayapuram N, Ahuja U, Thony-Meyer L, Grienenberger JM, Bonnard G (2005) AtCCMH, an essential component of the *c*-type cytochrome maturation pathway in Arabidopsis mitochondria, interacts with apocytochrome *c*. Proc Natl Acad Sci USA 102:16113–16118

Millar AH, Eubel H, Jänsch L, Kruft V, Heazlewood JL, Braun HP (2004) Mitochondrial cytochrome *c* oxidase and succinate dehydrogenase complexes contain plant specific subunits. Plant Mol Biol 56:77–90

Møller IM (2001) Plant mitochondria and oxidative stress: electron transport, NADPH turnover, and metabolism of reactive oxygen species. Annu Rev Plant Physiol Plant Mol Biol 52:561–591

Ner-Gaon H, Halachmi R, Savaldi-Goldstein S, Rubin E, Ophir R, Fluhr R (2004) Intron retention is a major phenomenon in alternative splicing in Arabidopsis. Plant J 39:877–885

Nobrega MP, Bandeira SC, Beers J, Tzagoloff A (2002) Characterization of COX19, a widely distributed gene required for expression of mitochondrial cytochrome oxidase. J Biol Chem 277:40206–40211

Orozco-Cardenas M, Ryan CA (1999) Hydrogen peroxide is generated systemically in plant leaves by wounding and systemin via the octadecanoid pathway. Proc Natl Acad Sci USA 96: 6553–6557

Pilon M, Abdel-Ghany SE, Cohu CM, Gogolin KA, Ye H (2006) Copper cofactor delivery in plant cells. Curr Opin Plant Biol 9:256–263

Rao MV, Paliyath G, Ormrod DP, Murr DP, Watkins CB (1997) Influence of salicylic acid on H_2O_2 production, oxidative stress, and H_2O_2-metabolizing enzymes. Salicylic acid-mediated oxidative damage requires H_2O_2. Plant Physiol 115:137–149

Rigby K, Zhang L, Cobine PA, George GN, Winge DR (2007) Characterization of the cytochrome *c* oxidase assembly factor Cox19 of *Saccharomyces cerevisiae*. J Biol Chem 282: 10233–10242

Rissler M, Wiedemann N, Pfannschmidt S, Gabriel K, Guiard B, Pfanner N, Chacinska A (2005) The essential mitochondrial protein Erv1 cooperates with Mia40 in biogenesis of intermembrane space proteins. J Mol Biol 353:485–492

Rosenzweig AC (2002) Metallochaperones: bind and deliver. Chem Biol 9:673–677

Sedmak J, Grossberg S (1977) A rapid, sensitive, and versatile assay for protein using Coomassie brilliant blue G-250. Anal Biochem 79:544–552

Thompson JD, Higgins DG, Gibson TJ (1994) CLUSTAL W: improving the sensitivity of progressive multiple sequence alignment through sequence weighting, positions-specific gap penalties and weight matrix choice. Nucleic Acids Res 22: 4673–4680

Wang J, Zhang H, Allen RD (1999) Overexpression of an Arabidopsis peroxisomal ascorbate peroxidase gene in tobacco increases protection against oxidative stress. Plant Cell Physiol 40: 725–732

Welchen E, Chan RL, Gonzalez DH (2002) Metabolic regulation of genes encoding cytochrome *c* and cytochrome *c* oxidase subunit Vb in Arabidopsis. Plant Cell Environ 25:1605–1615

Welchen E, Chan RL, Gonzalez DH (2004) The promoter of the Arabidopsis nuclear gene *COX5b-1*, encoding subunit 5b of the mitochondrial cytochrome *c* oxidase, directs tissue-specific expression by a combination of positive and negative regulatory elements. J Exp Bot 55:1997–2004

Welchen E, Gonzalez DH (2005) Differential expression of the Arabidopsis cytochrome *c* genes *Cytc-1* and *Cytc-2*: evidence for the involvement of TCP-domain protein binding elements in anther- and meristem-specific expression of the *Cytc-1* gene. Plant Physiol 139:88–100

Wintz H, Fox T, Vulpe C (2001) Responses of plants to iron, zinc and copper deficiencies. Biochem Soc Trans 30:766–768

Zabaleta E, Heiser V, Grohmann L, Brennicke A (1998) Promoters of nuclear-encoded respiratory chain complex I genes from *Arabidopsis thaliana* contain a region essential for anther/pollen-specific expression. Plant J 15:49–59